Unsteady Aerodynamic Simulation of a Floating Offshore Wind Turbine with Oscillating Pitch Motion

Ping Cheng, Yong Ai and Decheng Wan*
State Key Laboratory of Ocean Engineering, School of Naval Architecture, Ocean and Civil Engineering,
Shanghai Jiao Tong University, Collaborative Innovation Center for Advanced Ship and Deep-Sea Exploration,
Shanghai, China
*Corresponding author: dcwan@sjtu.edu.cn

ABSTRACT

The aerodynamic performance of the floating offshore wind turbines is much more complex than that of bottom-fixed wind turbines because of the motions of the supporting platform. In this paper, the unsteady aerodynamic performance of the NREL-5MW Baseline wind turbine with periodical pitch motions of its supporting platform is investigated. The three-dimensional Reynolds Averaged Navier-Stokes equations are solved for the aerodynamic numerical simulation. The naoe-FOAM-os-SJTU solver, which is based on OpenFOAM and overset grid technique, is employed. From the simulation, the time series of the unsteady torque and thrust are obtained, the detailed information of the wake flow field is also available to clarity the detailed flow filed information. The simulation results show that the pitch motion has significant effect on the aerodynamic forces and moments of the rotor, and the effect improves obviously when the amplitude of the pitch motion increases. The tower impacts are also analyzed in this paper.

KEY WORDS: periodical pitch motion; overset grid technology; naoe-FOAM-os-SJTU solver; tower impacts.

INTRODUCTION

Wind energy, which is renewable and sustainable, represents a potential to solve the energy and environment crisis, especially for the coastal countries which have enormous ocean wind energy resource. With special and strong advantages over onshore wind turbines, floating offshore wind turbines (FOWT) become more and more attractive. The environment loads on FOWTs become much more complex. Among the complex environment loads, besides the aerodynamic loads on the wind turbine, the hydrodynamic loads on the floating platform of FOWTs are of great significance.

Nowadays several FOWT programs have been in trial operation in some areas. Different from the platform used in the traditional oil and gas engineering, there is a wind turbine installed above the platform in FOWTs through a vertical tower, which affects the hydrodynamic performance of the platform with an unsteady aerodynamic loads of the turbine. The majority of the nowadays software for analyzing the FOWTs has advanced aerodynamics and limited hydrodynamics, because they were developed from analysis tools for onshore wind turbines. So, much attention has been paid to the hydrodynamic simulation of the supporting system of the FOWT in this paper.

There are three types of floating foundations which are widely used as the supporting system of the FOWTs: the tension leg platform (TLP), the spar platform and semi-submersible platform[1]. Sclavounos[2] studied on the hydrodynamic simulation of a TLP platform which is moored to gravity anchors, and obtained the linear and nonlinear wave loads on the platform with the methods which were developed for the design of oil and gas offshore platforms. Karimirad[3] studied on the hydrodynamic simulation of a spar type platform of FOWT, and got the extreme responses for the ultimate limit state design considering the coupled wave and wind induced motion and structural response in harsh condition. Kvittem[4] studied on hydrodynamic simulation of a semi-submersible platform used in FOWT, and examined the dynamic response of the platform based on different hydrodynamic theories.

The semi-submersible floating system for Phase II of OC4[5] is chosen as the simulation model in this paper. The Offshore Code Comparison Collaboration Continuation (OC4) project, which was formed in 2010 under the International Energy Agency Wind Task 30, is a project to verify the accuracy of the simulation tools and codes for the offshore wind turbine[6]. In this paper, the focus is on the

hydrodynamic simulation of the semi-submersible floating system coupled with the mooring system. To take the impacts of the wind turbine into consideration, the NREL offshore 5-MW baseline wind turbine[7] is simplified into equivalent unsteady forces and moments which are obtained in unsteady aerodynamic simulation of the wind turbine.

In this paper, the unsteady hydrodynamic analysis of the semi-submersible floating wind system for Phase II of the OC4 project with mooring system is carried out. The simulations are conducted with our in-house code naoe-FOAM-SJTU based on the open source code OpenFOAM. The finite volume method (FVM) is employed for solving Reynolds-Averaged Navier-Stokes (RANS) equations. The SST $k-\omega$ model[8] is chosen as the turbulence model. The Pressure-Implicit with Splitting of Operations algorithm (PISO) is used to solve the pressure-velocity coupling equation. The impact of the wind turbine is simplified into equivalent unsteady forces and moments. The forces and moments, as well as the motions of the floating system are generated by the naoe-FOAM-SJTU solver. The simulation results are compared with those obtained without impacts of the wind turbine. And proper discussions on the impact of the wind turbine are presented.

MATHEMATICAL MODEL AND NUMERICS

Governing Equations

The governing equation solved in this paper is the incompressible Reynolds-Average Navier-Stokes (RANS) equations which can be written as:

$$\frac{\partial U_i}{\partial x_i} = 0 \tag{1}$$

$$\frac{\partial U_i}{\partial t} + \frac{\partial}{\partial x_j}\left(U_i U_j\right) = -\frac{1}{\rho}\frac{\partial P}{\partial x_i} + \frac{\partial}{\partial x_j}\left(\nu\frac{\partial U_i}{\partial x_j} - \overline{u_i' u_j'}\right) \tag{2}$$

Where U is the velocity of flow; ρ is the density of the fluid; p is the pressure; ν is the kinematic viscosity.

To solve the above two equations, the k-ω SST turbulence model[8] is employed, in which the turbulent kinetic energy k and the turbulent dissipation rate ω can be described as:

$$\frac{\partial}{\partial t}(\rho k) + \frac{\partial}{\partial x_i}(\rho k u_i) = \frac{\partial}{\partial x_j}(\Gamma_k \frac{\partial k}{\partial x_j}) + G_k - Y_k + S_k \tag{3}$$

$$\frac{\partial}{\partial t}(\rho \omega) + \frac{\partial}{\partial x_i}(\rho \omega u_i) = \frac{\partial}{\partial x_j}(\Gamma_\omega \frac{\partial \omega}{\partial x_j}) + G_\omega - Y_\omega + D_\omega + S_\omega \tag{4}$$

Where, Γ_k and Γ_ω are the effective diffusion coefficients for the turbulent kinetic energy k and the turbulent

dissipation rate ω respectively, G_k and G_w are turbulence generation terms, Y_k and Y_w are turbulent dissipation terms, D_w is the cross-diffusion term for ω, S_k and S_w are the source term.

SIMULATION SETUP

Overset Grid Technique

The overset grid technique is used in this paper with our in-house code naoe-FOAM-os-SJTU[9], which is compiled by implementing the overset grid technique into the OpenFOAM-based solver naoe-FOAM-SJTU [10,11].

Using overset grid technique, the separate overlapping grids for each part with independent motion are allowed, which makes it a good method for simulation of large amplitude motion problems. And the connection among grids of each part is built by interpolation at appropriate cells or points using DCI (domain connectivity information) which is produced by SUGGAR++[12,13]. There are four main steps when using DCI in the overset grid technique: The first step is to find out the hole cells which are located outside the simulation domain or of no interest, and exclude them from computation. As shown in Fig.1, in each overset grid, there exist series of cells around hole cells named fringe cells, and for each fringe cell there are several donor cells which provide information from the donor grids, so the second step is to seek for the donor grids of each fringe cell and get information from the donor grids. The third step is to obtain the value of a variable ϕ of the fringe cell by interpolation using Eq.1 from the donor cells find in the second step.

$$\phi_I = \sum_{i=1}^{n} \omega_i \cdot \phi_i \tag{5}$$

Where ϕ_I is the value of a variable ϕ of the fringe cell, ϕ_i is the value for the ith donor cell, ω_i is the weight coefficient, which is dimensionless and follows the condition shown in Eq.2:

$$\sum_{i=1}^{n} \omega_i = 1 \tag{6}$$

And the last step is to optimize the overlapping area and improve the accuracy of interpolation.
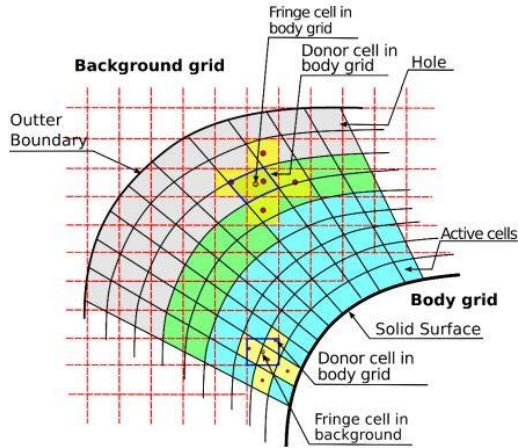
Fig. 1 Diagram of Overset Grid

Geometry model and grids

Phase II of OC4 project involving modeling of NREL 5MW Baseline Wind Turbine with the semi-submersible floating system[5,7] is chosen in this paper, which is shown below in Fig.2.
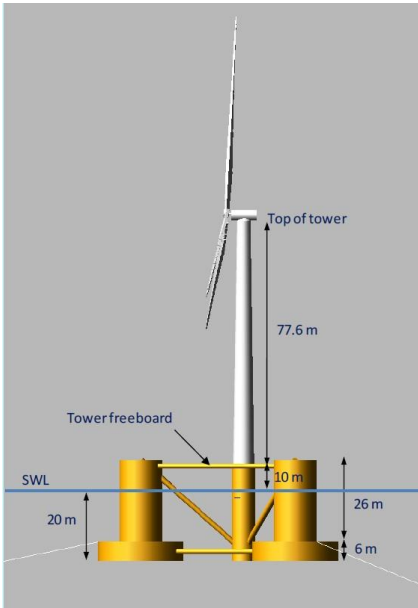

Fig. 2 The Phase II of OC4 floating wind turbine

As shown in Fig.2, The Phase II of OC4 floating wind turbine consists of two main parts: the turbine with tower in air and the semi-submersible platform with mooring lines in water. In this paper, the hydrodynamic performance of the floating platform is not computed directly, but its impact on the wind turbine is considered by simplified the motion of the platform as a prescribed sinusoidal motion in pitch direction.

Table.1 gives some properties of the NREL 5MW Baseline Wind Turbine and tower.

Table 1. Summary of Properties the NREL 5MW Baseline Wind Turbine and Tower

Rating	5MW
Rotor Orientation	Upwind
Rotor Diameter / Hub Diameter	126m / 3m
Hub Height	90m
Maximum Rotor / Generator Speed	12.1rpm / 1,173.7rpm
Length of Blade	61.5m
Height of Tower above Ground	87.6m

With these structural properties and the detailed data of blade [14], the structural model is built, which is shown in Fig.3. According to the structural properties listed in Table.1, the simulation domain is generated as a cylinder, which is shown in Fig.3. The radius the cylinder domain is about 2R, where R is the radius of the rotor, and length is 240m, which is about 4R. The distance between the model and the inlet boundary is 60m, and the distance between the model and the outlet boundary is 180m. To improve the simulation accuracy, refinement of the mesh around turbine and tower is necessary, and proper mesh refinement in the wake flow field is also very important to capture the flow information in the wake flow.

To use the overset grid technique, three overlapping meshes are generated separately, which are the background mesh of the simulation domain generated with ICEM-CFD, and two overlapping grids for the rotor and tower respectively generated with snappyHexMesh supplied with OpenFOAM.
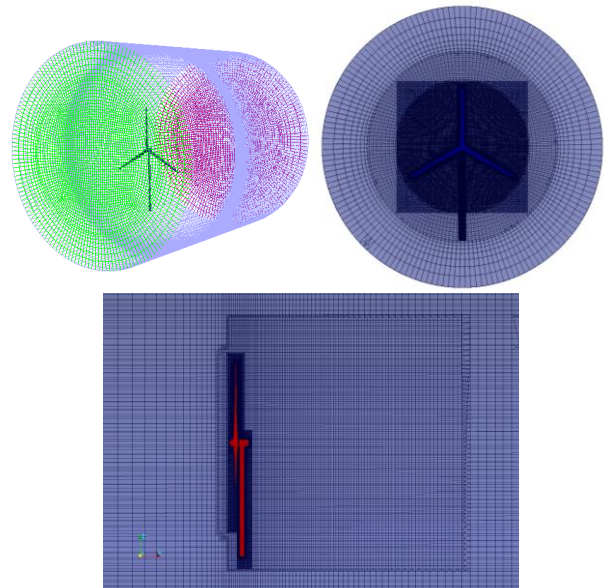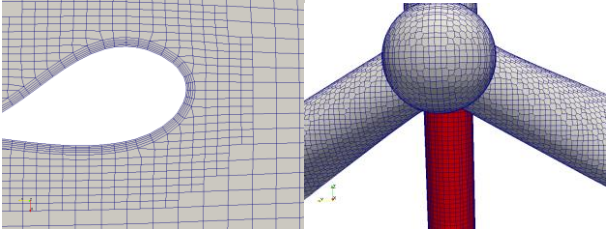
Fig. 3 Geometry Model and Grid Structure

Simulation Cases

In this paper, the aerodynamic simulation of the wind turbine is conducted with the impact of prescribed sinusoidal motion of the floating platform both in pitch directions. There are three cases selected in this paper, which are listed in Table.2. And the wind speed is set to the rated wind speed U=11.4m/s in all these simulations.

Table 2. Simulation Cases

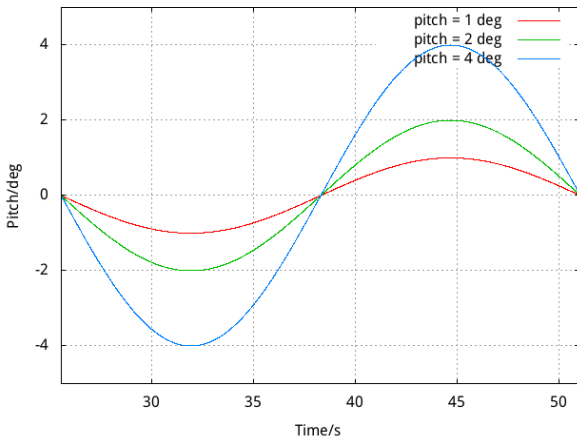|	Pitch (deg)
Case1	1*sin(0.246*t)
Case2	2*sin(0.246*t)
Case3	4*sin(0.246*t)

Fig. 4 Periodic Motion of the Turbine

Fig.4 shows the prescribed motion of the platform in one period in each case, in which the vertical axis shows the motion of the platform, and the horizontal axis shows the time value. The period of the platform pitch motion is 25.4s, which is about 5.15 times of the rotating period of rotor.

RESULTS AND DISCUSSION

Rotor Thrust and Torque

From the simulation, the time history of unsteady thrust and torque of the wind turbine are obtained. The time history of thrust and torque are shown in Fig5-6.

The non-dimensional treatment is done on the thrust and torque results by dividing the thrust or torque by the mean value.
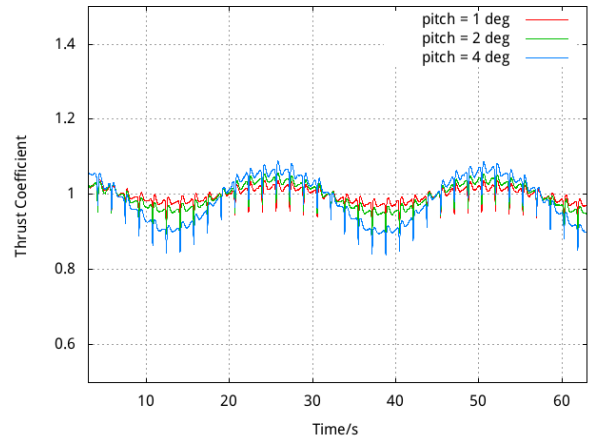

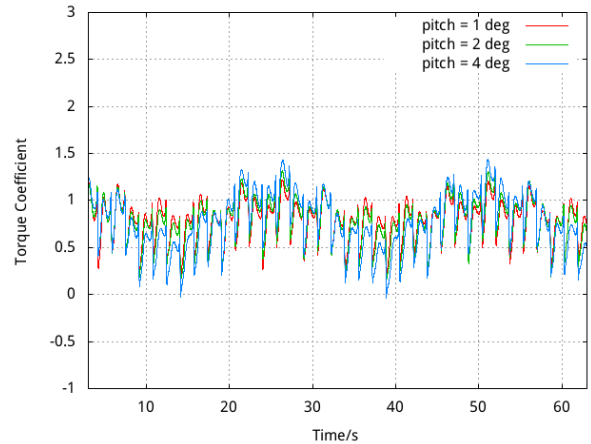Fig. 5 Thrust Coefficient of the Turbine

Fig. 6 Torque Coefficient of the Turbine

Fig.5 shows the time history of the thrust with predicted pitch motion. When comparing the three thrust figures in Fig.5, it is easy to find that the pitch motion has significant effects on the aerodynamic forces of the rotor. And the effect of the platform motion improves obviously when the amplitude of the pitch motion increase. There is an interesting phenomenon that three valleys can be observed during each one rotating period of rotor, which is caused by the tower effects, which was introduced in our earlier study [15].

Fig6 shows the time history of the torque coefficient. Similar conclusions can be made from the three curves of torque. Pitch motion of the platform has significant effects on the torque. The effects of the platform motion improve obviously when the amplitude of the motion increase. And the three valleys during each rotating period caused by the tower effects can also be observed.

Wake Flow

The wake vortex structure is a very important index in the aerodynamic analysis of wind turbine, because the wake vortex near the blades has great influence on the aerodynamic properties of the blades. To get a proper wake vortex visualization result, the second invariant of the velocity gradient tensor Q[16] is used to capture the iso-surface of the vortex, which is:

$$Q = \frac{1}{2}(\Omega_{ij} \times \Omega_{ij} - S_{ij} \times S_{ij}) \qquad (7)$$

In which Ω_{ij} is the strength of the vortex, and S_{ij} is the shear strain rate.

The evolution of wake vortex at different time (0, 1/8T, 2/8T, 3/8T, 4/8T, 5/8T, 6/8T, 7/8T) of a pitch period is illustrated in Fig.7. And the velocity distribution on the cross slice of the simulation domain is also combined in Fig.7 at each time.

(a) 0   (b) 1/8T

(c) 2/8T   (d) 3/8T

(e) 4/8T   (f) 5/8T
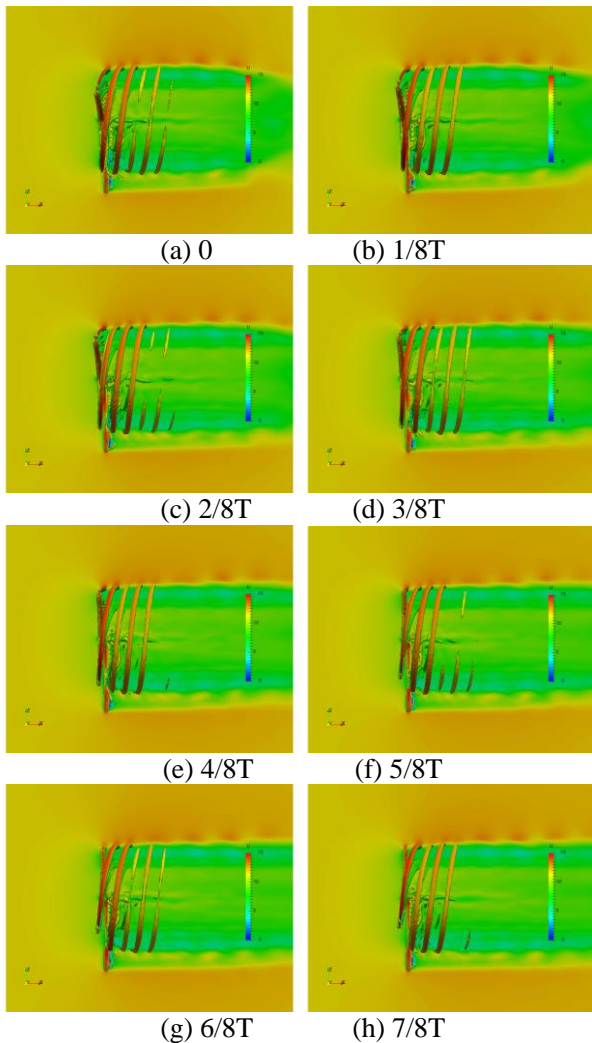
(g) 6/8T   (h) 7/8T

Fig. 7 Flow Structure of Wake Flow

Comparing the wake flow structures at different time

in Fig.7, we can figure out that the wind speed decreases a lot when passing the blades, which can be seen from the green parts in Fig.7, and the velocity reduced field should be a cylinder. The motion of the platform makes the wake velocity-reduced cylinder pitches at the same time. The pitch motion also makes the distances between two adjacent iso-surface of wake vortex change with the the same pitch motion period.

Tower Impact

As mentioned above, there are three valleys during each rotating period of the rotor in both Fig.5 and Fig.6. So pressure distributions on the horizontal slice which is 30m below the rotor center at three times are shown in figure.8. In Fig.8, the relative positions of the blades to tower are shown in the three right figures. The right figure in Fig.8(b) shows that at that time, one of the turbine is overlapping the tower, and the pressure in front of the tower becomes much lower than that at other times, and the pressure distribution around the blade slice is also changed, so the both thrust and torque changes at the same time.
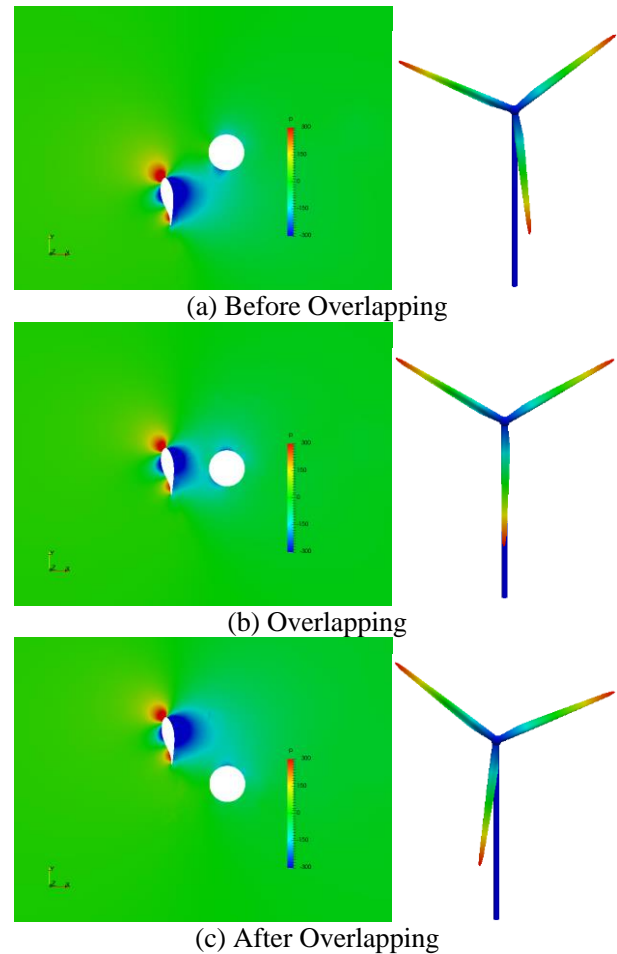

(a) Before Overlapping

(b) Overlapping

(c) After Overlapping

Fig. 8 Pressure Distribution on A horizontal slice

CONCLUSIONS

Both the time history curve of thrust and torque tell that the pitch motion of the platform makes the thrust and torque forces oscillating with the same period as the pith motion, and the improvement of the amplitude of the pitch motion will cause the increase of the amplitude of the oscillating of forces. With impacts of tower, three valleys are observed in both thrust and torque curves during one rotating period.

ACKNOWLEDGEMENTS

REFERENCES

[1] Sclavounos, P. (2008). Floating offshore wind turbines. Marine Technology Society Journal, 42(2), 39-43.

[2] Sclavounos P D, Lee S, DiPietro J, et al. (2010) Floating offshore wind turbines: tension leg platform and taught leg buoy concepts supporting 3-5 MW wind turbines. European wind energy conference EWEC, 20-23.

[3] Karimirad M, Moan T. (2011). Extreme dynamic structural response analysis of catenary moored spar wind turbine in harsh environmental conditions. Journal of offshore mechanics and Arctic engineering, 133(4): 041103.

[4] Kvittem M I, Bachynski E E, Moan T. (2012). Effects of hydrodynamic modelling in fully coupled simulations of a semi-submersible wind turbine. Energy Procedia, 24: 351-362.

[5] Robertson A, Jonkman J, Masciola M, et al. (2012). Definition of the Semisubmersible Floating System for Phase II of OC4. Offshore Code Comparison Collaboration Continuation (OC4) for IEA Task, 30.

[6] Robertson A, Jonkman J, Musial W, et al. (2013). Offshore Code Comparison Collaboration, Continuation: Phase II Results of a Floating Semisubmersible Wind System. EWEA Offshore, Frankfurt, Germany, no. NREL/CP-5000-60600.

[7] Jonkman, J. M., Butterfield, S., Musial, W., and Scott, G. (2009). Definition of a 5-MW reference wind turbine for offshore system development. Golden, CO: National Renewable Energy Laboratory.

[8] Menter, FR (1994). Two-equation eddy-viscosity turbulence models for engineering applications [J]. AIAA journal, 32(8): 1598-1605.

[9] Shen ZR, Wan DC, Carrica, PM (2015). Dynamic overset grids in OpenFOAM with application to KCS self-propulsion and maneuvering [J]. Ocean Engineering, 108: 287-306.

[10] Shen, ZR., Cao, HJ, Wan, DC (2012). Manual of CFD solver for ship and ocean engineering flows: naoe-FOAM-SJTU. Technical Report for Solver Manual, Shanghai Jiao Tong University.

[11] Shen, ZR, Wan, DC (2013). RANS computations of added resistance and motions of a ship in head waves. Int. J. Offshore Polar Eng. 23 (4), 263–271.

[12] Carrica, PM, Huang, J, Noack, RW, Kaushik, D, Smith, B, Stern, F (2010). Large-scale DES computations of the forward speed diffraction and pitch and heave problems for a surface combatant [J]. Computers & Fluids, 39(7): 1095-1111.

[13] Noack, RW (2005). SUGGAR: a general capability for moving body overset grid assembly [C]. Proceedings of the 17th AIAA Computational Fluid Dynamics Conference, American Institute of Aeronautics and Astronautics, Toronto, Ontario, Canada.

[14] Lindenburg, C (2002). Aeroelastic modelling of the LMH64-5 blade [J]. Energy Research Center of the Netherlands, Technical Report No. DOWEC-02-KL-083/0, DOWEC 10083_001.

[15] Cheng, P, Wan, DC (2015). Numerical Simulations of Complex Aerodynamic Flows around NREL Offshore 5-MW Baseline Wind Turbine[C]. Proceedings of the 9th International Workshop on Ship and Marine Hydrodynamics, 26 – 28 August 2015, Glasgow, UK.

[16] Digraskar, DA (2010). Simulations of flow over wind turbines [J].